Proceedings of the 17th World Congress
The International Federation of Automatic Control
Seoul, Korea, July 6-11, 2008

Ship Formation Control: A Guided Leader-Follower Approach ⋆

Morten Breivik * **Vegard E. Hovstein** ** **Thor I. Fossen** *

* *{Centre for Ships and Ocean Structures, Department of Engineering Cybernetics}, Norwegian University of Science and Technology, NO-7491 Trondheim, Norway.*
E-mails: {morten.breivik, fossen}@ieee.org
** *Maritime Robotics, NO-7010, Trondheim, Norway.*
E-mail: vegard.hovstein@maritimerobotics.com

Abstract: This paper considers the topic of formation control for fully actuated ships. Within a leader-follower framework, a so-called guided formation control scheme is developed by means of a modular design procedure inspired by concepts from integrator backstepping and cascade theory. Control, guidance, and synchronization laws ensure that each individual formation member is able to converge to and maintain its assigned formation position such that the overall formation is able to assemble and maintain itself while traversing an arbitrary, regularly parameterized path that is chosen by a formation control designer. A key novelty of the approach is the derivation of guidance laws that are applicable to off-path traversing of curved paths. The helmsman-like transient motion behavior associated with the scheme is illustrated through a computer simulation involving three fully actuated ships.

1. INTRODUCTION

Formation control technology plays an increasingly important role for commercial, scientific, and military purposes. Today, relevant applications can be found everywhere; at sea, on land, in the air, and in space. At sea, the subject of formation control has been important for centuries. In old times, groups of warships had to be controlled during naval battles. In both world wars, it was pivotal for merchant ships to travel in convoys. Current applications include underway ship replenishment, towing of large structures at sea, and surveying of hydrocarbons. In the future, more sophisticated concepts will emerge, facilitated by new sensor, communication, and computer technology. Formations will become increasingly autonomous, consisting of fully autonomous marine craft that must operate in so-called dirty, dull, and dangerous environments. The vessels can act as scouts, nodes in communication and sensor networks, or elements within battlegroups. Ultimately, multi-vehicle operations render possible tasks that no single vehicle can solve, as well as increase operational robustness toward individual failures.

A main pillar in the Norwegian economy is oil and gas production. Hence, a principal motivation for Norwegian research efforts concerns the commercial offshore market, where formation control technology is expected to play a key role in future hydrocarbon exploration and exploitation. Such technology can contribute to reduced personnel costs, increased personnel safety, extended weather window (of operations), increased operational precision, and more environmentally friendly operations.

⋆ This work was supported by the Norwegian Research Council through the Centre for Ships and Ocean Structures and through the MAROFF grant 175977: Unmanned Surface Vehicle.

1.1 Previous Work

Research within formation control theory can be divided into two main categories; the analytic and the algorithmic. The analytic category represents those approaches that are most readily analyzed by mathematical tools, and include both leader-follower methods and virtual structure schemes. Conversely, the algorithmic category represents those approaches that are not easily analyzed mathematically, but have to be numerically simulated by means of a computer in order to investigate their emergent behavior. So-called behavior-based methods belong to this category.

During recent years, the marine control community has focused considerably on formation control concepts. Most of the work seems to have been performed within a leader-follower framework, e.g., in (Encarnação and Pascoal 2001), where an autonomous underwater vehicle (AUV) tracks the planar projection of a surface craft onto its nominal path, while the surface craft follows its own path at sea; in (Skjetne *et al.* 2002), where formation control of multiple so-called maneuvering systems yields a robust scheme with dynamic adjustment to the weakest link of the formation; in (Lapierre *et al.* 2003), where coordination of two AUVs is achieved by augmenting a path parameter synchronization algorithm to the controller of the follower vehicle; in (Aguiar *et al.* 2006), where multiple AUVs are coordinated along spatial paths despite communication constraints; in (Kyrkjebø and Pettersen 2006), where surface vessels are synchronized through a leader-follower scheme; and in (Pavlov *et al.* 2007), where formation control of underactuated surface vessels moving along straight lines are considered. Work related to virtual structures is reported in (Fiorelli *et al.* 2004), where cooperative control of AUVs is achieved through the use of virtual leaders and artificial potentials, considering the formation as a

rigid-body geometric structure; and in (Ihle *et al.* 2005), where the approach is rooted in analytical mechanics for multi-body dynamics, facilitating a flexible and robust formation control scheme where the geometric constraints of a virtual structure are enforced by feedback control. Also, research in the vein of behavioral methods can be found in (Arrichiello *et al.* 2006), where marine surface vessels move in formation while avoiding collisions with environmental obstacles. Finally, the anthologies (Kumar *et al.* 2005) and (Pettersen *et al.* 2006) report state-of-the-art concepts for a broad number of formation control scenarios.

1.2 Main Contribution

The main contribution of this paper is a concept named *guided formation control*. Developed within a leader-follower framework, the scheme is based on principles from integrator backstepping design (Krstić *et al.* 1995) as well as theory for nonlinear time-varying cascades (Panteley *et al.* 1998). The proposed design procedure for each individual ship is completely modular, and consists of three distinct steps where control, guidance, and synchronization laws are sequentially derived. A key novelty of the approach is the derivation of the required guidance laws for off-path traversing of curved paths. These laws also ensure that each formation member displays helmsman-like motion behavior during the transient formation assembly phase. The guided approach can be used with both centralized and decentralized formation control strategies, and is illustrated through a decentralized strategy where no inter-vessel communication is required.

2. GUIDED FORMATION CONTROL

In what follows, when considering a vector $\mathbf{x}$ that is parameterized by a time-varying scalar variable ϖ (i.e., $\mathbf{x}(\varpi(t))$), the time derivative of $\mathbf{x}$ is denoted $\dot{\mathbf{x}}$, while the partial derivative with respect to ϖ is denoted $\mathbf{x}' = \frac{\partial \mathbf{x}}{\partial \varpi}$. Also, $|\cdot|$ represents both the Euclidean vector norm and the induced matrix norm.

2.1 Ship Dynamic Model

A 3 degree-of-freedom (DOF) dynamic model of the horizontal surge, sway, and yaw modes can be found in (Fossen 2002), and consists of the kinematics

$$\dot{\boldsymbol{\eta}} = \mathbf{R}(\psi)\boldsymbol{\nu}, \tag{1}$$

and the kinetics

$$\mathbf{M}\dot{\boldsymbol{\nu}} + \mathbf{C}(\boldsymbol{\nu})\boldsymbol{\nu} + \mathbf{D}(\boldsymbol{\nu})\boldsymbol{\nu} = \boldsymbol{\tau} + \mathbf{R}(\psi)^\top \mathbf{b}, \tag{2}$$

where $\boldsymbol{\eta} \triangleq [x, y, \psi]^\top \in \mathbb{R}^3$ represents the earth-fixed position and heading; $\boldsymbol{\nu} \triangleq [u, v, r]^\top \in \mathbb{R}^3$ represents the vessel-fixed velocity; $\mathbf{R}(\psi) \in SO(3)$ is the transformation matrix

$$\mathbf{R}(\psi) \triangleq \begin{bmatrix} \cos\psi & -\sin\psi & 0 \\ \sin\psi & \cos\psi & 0 \\ 0 & 0 & 1 \end{bmatrix} \tag{3}$$

that transforms from the vessel-fixed BODY frame to the earth-fixed NED frame; $\mathbf{M}$ is the inertia matrix; $\mathbf{C}(\boldsymbol{\nu})$ is the centrifugal and coriolis matrix; while $\mathbf{D}(\boldsymbol{\nu})$ is the hydrodynamic damping matrix. The system matrices satisfy the properties $\mathbf{M} = \mathbf{M}^\top > 0$, $\mathbf{C} = -\mathbf{C}^\top$ and $\mathbf{D} > 0$. The vessel-fixed propulsion forces and moment is represented by $\boldsymbol{\tau} \triangleq [\tau_{\mathrm{X}}, \tau_{\mathrm{Y}}, \tau_{\mathrm{N}}]^\top \in \mathbb{R}^3$, corresponding to a fully actuated ship. Full actuation means that all 3 DOFs can be controlled independently at the same time, i.e., the linear velocity is independent of the vessel heading. Finally, $\mathbf{b}$ represents low-frequency, earth-fixed environmental disturbances.

2.2 Formation Control Scenario

This work considers formation control within a leader-follower framework, where a formation structure is defined relative to a virtual formation leader. It is assumed that the formation control designer can choose both the path to be traversed by the leader, the temporal motion of the leader, as well as the geometric formation structure defined relative to the leader.

Consequently, consider a planar path continuously parameterized by a scalar variable $\varpi \in \mathbb{R}$, such that the position of a point belonging to the path is represented by $\mathbf{p}_{\mathrm{p}}(\varpi) \in \mathbb{R}^2$. Thus, the path is a one-dimensional manifold that can be expressed by the set

$$\mathcal{P} \triangleq \left\{ \mathbf{p} \in \mathbb{R}^2 \mid \mathbf{p} = \mathbf{p}_{\mathrm{p}}(\varpi)\ \forall \varpi \in \mathbb{R} \right\}. \tag{4}$$

Then, represent the virtual formation leader by $\mathbf{p}_{\mathrm{l}}(t) \triangleq \mathbf{p}_{\mathrm{p}}(\varpi_{\mathrm{l}}(t))$. The leader traverses the path by adhering to the speed profile $U_{\mathrm{l}}(\varpi_{\mathrm{l}})$, implemented through

$$\dot{\varpi}_{\mathrm{l}} = \frac{U_{\mathrm{l}}(\varpi_{\mathrm{l}})}{\left|\mathbf{p}'_{\mathrm{p}}(\varpi_{\mathrm{l}})\right|}, \tag{5}$$

since $|\dot{\mathbf{p}}_{\mathrm{l}}| = \left|\mathbf{p}'_{\mathrm{p}}(\varpi_{\mathrm{l}})\right| \dot{\varpi}_{\mathrm{l}} = U_{\mathrm{l}}(\varpi_{\mathrm{l}})$, where $U_{\mathrm{l}}(\varpi_{\mathrm{l}}) \in [U_{\mathrm{l,min}}, U_{\mathrm{l,max}}]$, $U_{\mathrm{l,min}} > 0$ (non-negative by definition).

Furthermore, consider a formation consisting of n members, each uniquely identified through the index set $\mathcal{I} = \{1, ..., n\}$. The assigned formation position for member i is represented by $\mathbf{p}_{\mathrm{f,i}}(t)$, which is related to the formation leader through a chosen geometric assignment (defined in local, path-tangential coordinates relative to the leader). By design, we ensure that no formation positions are identical, i.e., $\mathbf{p}_{\mathrm{f,i}} \neq \mathbf{p}_{\mathrm{f,j}}\ \forall i \neq j$, where $i, j \in \mathcal{I}$.

Problem Statement The formation control problem for fully actuated ships can be stated by

$$\lim_{t\to\infty} \left(\boldsymbol{\eta}_{\mathrm{i}}(t) - \boldsymbol{\eta}_{\mathrm{f,i}}(t)\right) = \mathbf{0}\ \forall i \in \mathcal{I}, \tag{6}$$

where $\boldsymbol{\eta}_{\mathrm{i}}(t)$ represents the ith formation member, and $\boldsymbol{\eta}_{\mathrm{f,i}}(t) \triangleq \left[\mathbf{p}_{\mathrm{f,i}}^\top(t), \psi_{\mathrm{d,i}}(t)\right]^\top \in \mathbb{R}^3$, where $\psi_{\mathrm{d,i}}(t)$ can be any arbitrary desirable heading (typically the path-tangential orientation at $\mathbf{p}_{\mathrm{l}}(t)$) satisfying some auxiliary task objective. See Figure 1 for an illustration of the formation control concept under consideration.

2.3 Motion Control of Individual Formation Members

This section develops the control, guidance and synchronization laws that each formation member must employ in order to converge to its assigned position in the formation. The underlying concept is adapted from (Breivik *et al.* 2006), and entails a modular three-step, backstepping-inspired and cascaded-based design procedure.

Step 1: Control Loop Design Since the position of a vessel can be controlled through its linear velocity, we redefine the output space from the nominal 3 DOF position and heading to the 3 DOF linear velocity and heading (Fossen *et al.* 2003). Consequently, consider the positive definite and radially unbounded Control Lyapunov Function (CLF)

$$V_{\mathrm{g}} \triangleq \frac{1}{2}(z_\psi^2 + \mathbf{z}_\nu^\top \mathbf{M}\mathbf{z}_\nu + \tilde{\mathbf{b}}^\top \mathbf{\Gamma}^{-1}\tilde{\mathbf{b}}) \tag{7}$$

where we have

$$z_\psi \triangleq \psi - \psi_{\mathrm{d}} \tag{8}$$

and

$$\mathbf{z}_\nu \triangleq \boldsymbol{\nu} - \boldsymbol{\alpha}, \tag{9}$$

where $\boldsymbol{\alpha} \triangleq [\alpha_{\mathrm{u}}, \alpha_{\mathrm{v}}, \alpha_{\mathrm{r}}]^\top \in \mathbb{R}^3$ is a so-called vector of stabilizing functions (virtual inputs that become reference signals) yet to be designed. Also,

$$\tilde{\mathbf{b}} \triangleq \hat{\mathbf{b}} - \mathbf{b} \tag{10}$$

represents an adaptation error where $\hat{\mathbf{b}}$ is the estimate of $\mathbf{b}$, and by assumption $\dot{\mathbf{b}} = \mathbf{0}$. Finally, $\mathbf{\Gamma} = \mathbf{\Gamma}^\top > 0$ is the so-called adaptation gain matrix.

Subsequently, differentiate the CLF with respect to time to obtain

$$\begin{aligned}\dot{V}_{\mathrm{g}} &= z_\psi \dot{z}_\psi + \mathbf{z}_\nu^\top \mathbf{M}\dot{\mathbf{z}}_\nu + \tilde{\mathbf{b}}^\top \mathbf{\Gamma}^{-1}\dot{\tilde{\mathbf{b}}} \\ &= z_\psi(\dot{\psi} - \dot{\psi}_{\mathrm{d}}) + \mathbf{z}_\nu^\top \mathbf{M}(\dot{\boldsymbol{\nu}} - \dot{\boldsymbol{\alpha}}) + \tilde{\mathbf{b}}^\top \mathbf{\Gamma}^{-1}\dot{\hat{\mathbf{b}}},\end{aligned}$$

which is equal to

$$\dot{V}_{\mathrm{g}} = z_\psi(\mathbf{h}^\top \dot{\boldsymbol{\eta}} - \dot{\psi}_{\mathrm{d}}) + \mathbf{z}_\nu^\top(\mathbf{M}\dot{\boldsymbol{\nu}} - \mathbf{M}\dot{\boldsymbol{\alpha}}) + \tilde{\mathbf{b}}^\top \mathbf{\Gamma}^{-1}\dot{\hat{\mathbf{b}}}$$

by introducing

$$\mathbf{h} \triangleq [0, 0, 1]^\top. \tag{11}$$

Furthermore, recognizing that $\mathbf{h}^\top \dot{\boldsymbol{\eta}} = \mathbf{h}^\top \mathbf{R}\boldsymbol{\nu} = \mathbf{h}^\top \boldsymbol{\nu}$ and $\boldsymbol{\nu} = \mathbf{z}_\nu + \boldsymbol{\alpha}$, we obtain

$$\begin{aligned}\dot{V}_{\mathrm{g}} = z_\psi(\mathbf{h}^\top \boldsymbol{\alpha} - \dot{\psi}_{\mathrm{d}}) + \mathbf{z}_\nu^\top(\boldsymbol{\tau} - \mathbf{C}\boldsymbol{\nu} - \mathbf{D}\boldsymbol{\nu} - \mathbf{M}\dot{\boldsymbol{\alpha}}) + \\ \mathbf{z}_\nu^\top(\mathbf{R}^\top \mathbf{b} + \mathbf{h}z_\psi) + \tilde{\mathbf{b}}^\top \mathbf{\Gamma}^{-1}\dot{\hat{\mathbf{b}}},\end{aligned}$$

which results in

$$\begin{aligned}\dot{V}_{\mathrm{g}} = -k_\psi z_\psi^2 - \mathbf{z}_\nu^\top \mathbf{C}\mathbf{z}_\nu - \mathbf{z}_\nu^\top \mathbf{D}\mathbf{z}_\nu + \\ \mathbf{z}_\nu^\top(\boldsymbol{\tau} - \mathbf{C}\boldsymbol{\alpha} - \mathbf{D}\boldsymbol{\alpha} - \mathbf{M}\dot{\boldsymbol{\alpha}}) + \\ \mathbf{z}_\nu^\top(\mathbf{R}^\top \hat{\mathbf{b}} + \mathbf{h}z_\psi) + \tilde{\mathbf{b}}^\top \mathbf{\Gamma}^{-1}(\dot{\hat{\mathbf{b}}} - \mathbf{\Gamma}\mathbf{R}\mathbf{z}_\nu)\end{aligned}$$

since $\mathbf{b} = \hat{\mathbf{b}} - \tilde{\mathbf{b}}$, and when choosing the virtual input $\mathbf{h}^\top \boldsymbol{\alpha} = \alpha_{\mathrm{r}}$ as

$$\alpha_{\mathrm{r}} = \dot{\psi}_{\mathrm{d}} - k_\psi z_\psi, \tag{12}$$

where $k_\psi > 0$ is a constant. Since $\mathbf{z}_\nu^\top \mathbf{C}\mathbf{z}_\nu = 0$, by selecting the control input

$$\boldsymbol{\tau} = \mathbf{M}\dot{\boldsymbol{\alpha}} + \mathbf{C}\boldsymbol{\alpha} + \mathbf{D}\boldsymbol{\alpha} - \mathbf{R}^\top \hat{\mathbf{b}} - \mathbf{h}z_\psi - \mathbf{K}_\nu \mathbf{z}_\nu \tag{13}$$

where $\mathbf{K}_\nu = \mathbf{K}_\nu^\top > 0$ is a constant matrix, and by choosing the disturbance adaptation update law

$$\dot{\hat{\mathbf{b}}} = \mathbf{\Gamma}\mathbf{R}\mathbf{z}_\nu, \tag{14}$$

we finally obtain the negative semi-definite

$$\dot{V}_{\mathrm{g}} = -k_\psi z_\psi^2 - \mathbf{z}_\nu^\top(\mathbf{D} + \mathbf{K}_\nu)\mathbf{z}_\nu. \tag{15}$$

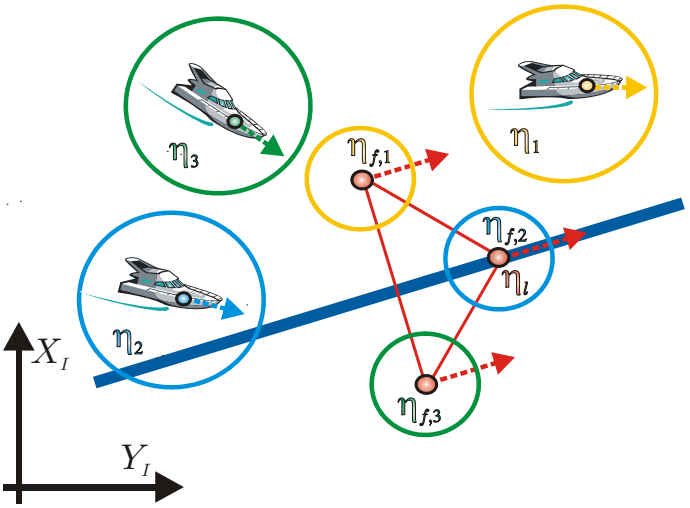

Fig. 1. A formation control scenario where 3 ships assemble and maintain a V-shaped formation along a straight-line path.

Considering the state vector $\mathbf{z}_{\mathrm{g}} \triangleq \left[z_\psi, \mathbf{z}_\nu^\top, \tilde{\mathbf{b}}^\top\right]^\top$, the following proposition can now be stated:

Proposition 1. The equilibrium point $\mathbf{z}_{\mathrm{g}} = \mathbf{0}$ is rendered uniformly globally asymptotically and locally exponentially stable (UGAS/ULES) by adhering to (12), (13) and (14) under the assumption that $\boldsymbol{\alpha}$ and $\dot{\boldsymbol{\alpha}}$ are uniformly bounded.

Proof. The proposed result follows by straightforward application of Theorem 1 in (Fossen *et al.* 2001). ■

Note that the stability property of Proposition 1 is known as global κ-exponential stability, as originally defined in (Sørdalen and Egeland 1995). In fact, global κ-exponential stability is the best stability property a physical system like a ship can achieve due to the limitations on its propulsion system. Also, note that the developed controller cannot achieve anything meaningful motionwise unless it is fed sensible reference signals, i.e., unless $\boldsymbol{\alpha}_{\mathrm{v}} \triangleq [\alpha_{\mathrm{u}}, \alpha_{\mathrm{v}}]^\top \in \mathbb{R}^2$ is purposefully defined. This task is the responsibility of the final two design steps.

Step 2: Guidance Loop Design We now design the required *orientation* of $\boldsymbol{\alpha}_{\mathrm{v}}$ such that a ship controlled by (13) and (14) attains its assigned formation position relative to the path (even though it may not be synchronized with the leader). This part contributes a key novelty to the scheme by deriving guidance laws that facilitate (singularity-free) off-path traversing of curved paths.

Consequently, consider the positive definite and radially unbounded CLF

$$V_{\tilde{\varepsilon}} \triangleq \frac{1}{2}\tilde{\boldsymbol{\varepsilon}}^\top \tilde{\boldsymbol{\varepsilon}}, \tag{16}$$

with

$$\tilde{\boldsymbol{\varepsilon}} \triangleq \boldsymbol{\varepsilon} - \boldsymbol{\varepsilon}_{\mathrm{f}} \tag{17}$$

and

$$\boldsymbol{\varepsilon} \triangleq \mathbf{R}_{\mathrm{C}}^\top(\mathbf{p} - \mathbf{p}_{\mathrm{c}}), \tag{18}$$

where $\mathbf{p}_{\mathrm{c}} \triangleq \mathbf{p}_{\mathrm{p}}(\varpi_{\mathrm{c}})$ represents a (virtual) *collaborator* point that cooperates with the ship as an intermediate path

attractor, such that the ship can converge to its assigned formation position relative to the path $\boldsymbol{\varepsilon}_\mathrm{f}$ irrespective of whether it has synchronized with the formation leader or not. Furthermore, the path-tangential reference frame at $\mathbf{p}_\mathrm{c}$ is termed the COLLABORATOR frame (**C**). To arrive at **C**, the INERTIAL frame (**I**) must be positively rotated an angle

$$\chi_\mathrm{c} \triangleq \arctan\left(\frac{y'_\mathrm{p}(\varpi_\mathrm{c})}{x'_\mathrm{p}(\varpi_\mathrm{c})}\right), \tag{19}$$

which can be represented by the rotation matrix

$$\mathbf{R}_\mathrm{C} \triangleq \begin{bmatrix} \cos\chi_\mathrm{c} & -\sin\chi_\mathrm{c} \\ \sin\chi_\mathrm{c} & \cos\chi_\mathrm{c} \end{bmatrix}, \tag{20}$$

$\mathbf{R}_\mathrm{C} \in SO(2)$. Hence, equation (18) represents the error vector between the ship and its collaborator decomposed in **C**. The local coordinates $\boldsymbol{\varepsilon} \triangleq [s, e]^\top$ consist of the *along-track error* s and the *cross-track error* e. By driving $\tilde{\boldsymbol{\varepsilon}}$ to zero, $\boldsymbol{\varepsilon}$ becomes equal to $\boldsymbol{\varepsilon}_\mathrm{f}$ such that the ship attains its assigned path-relative formation position. It is assumed that $\boldsymbol{\varepsilon}_\mathrm{f}$, $\dot{\boldsymbol{\varepsilon}}_\mathrm{f}$ and $\ddot{\boldsymbol{\varepsilon}}_\mathrm{f}$ are uniformly bounded, and typically $\dot{\boldsymbol{\varepsilon}}_\mathrm{f} = \ddot{\boldsymbol{\varepsilon}}_\mathrm{f} = \mathbf{0}$.

Now, differentiate the CLF in (16) along the trajectories of $\tilde{\boldsymbol{\varepsilon}}$ to obtain

$$\begin{aligned}
\dot{V}_{\tilde{\varepsilon}} &= \tilde{\boldsymbol{\varepsilon}}^\top \dot{\tilde{\boldsymbol{\varepsilon}}} \\
&= \tilde{\boldsymbol{\varepsilon}}^\top (\mathbf{S}_\mathrm{C}^\top \mathbf{R}_\mathrm{C}^\top (\mathbf{p} - \mathbf{p}_\mathrm{c}) + \mathbf{R}_\mathrm{C}^\top (\dot{\mathbf{p}} - \dot{\mathbf{p}}_\mathrm{c}) - \dot{\boldsymbol{\varepsilon}}_\mathrm{f}) \\
&= \tilde{\boldsymbol{\varepsilon}}^\top \left(\mathbf{S}_\mathrm{C}^\top \boldsymbol{\varepsilon} + \mathbf{R}_\mathrm{C}^\top \mathbf{v}^\mathrm{I} - \mathbf{v}_\mathrm{c}^\mathrm{C} - \dot{\boldsymbol{\varepsilon}}_\mathrm{f}\right) \\
&= \tilde{\boldsymbol{\varepsilon}}^\top \left(\mathbf{S}_\mathrm{C}^\top \tilde{\boldsymbol{\varepsilon}} + \mathbf{S}_\mathrm{C}^\top \boldsymbol{\varepsilon}_\mathrm{f} + \mathbf{R}_\mathrm{C}^\top \mathbf{v}^\mathrm{I} - \mathbf{v}_\mathrm{c}^\mathrm{C} - \dot{\boldsymbol{\varepsilon}}_\mathrm{f}\right) \\
&= \tilde{\boldsymbol{\varepsilon}}^\top \left(\mathbf{R}_\mathrm{C}^\top \mathbf{v}^\mathrm{I} - \mathbf{v}_\mathrm{c}^\mathrm{C} + \mathbf{S}_\mathrm{C}^\top \boldsymbol{\varepsilon}_\mathrm{f} - \dot{\boldsymbol{\varepsilon}}_\mathrm{f}\right),
\end{aligned}$$

where $\dot{\mathbf{R}}_\mathrm{C} = \mathbf{R}_\mathrm{C}\mathbf{S}_\mathrm{C}$ with $\mathbf{S}_\mathrm{C} = -\mathbf{S}_\mathrm{C}^\top \Rightarrow \tilde{\boldsymbol{\varepsilon}}^\top \mathbf{S}_\mathrm{C}^\top \tilde{\boldsymbol{\varepsilon}} = 0$, $\mathbf{v}^\mathrm{I} \triangleq \dot{\mathbf{p}}$ represents the linear velocity of the ship decomposed in **I**, and $\mathbf{v}_\mathrm{c}^\mathrm{C} \triangleq \mathbf{R}_\mathrm{C}^\top \dot{\mathbf{p}}_\mathrm{c} = [U_\mathrm{c}, 0]^\top$ ($U_\mathrm{c} = |\dot{\mathbf{p}}_\mathrm{c}|$) represents the linear velocity of the collaborator decomposed in **C**. Furthermore,

$$\begin{aligned}
\dot{V}_{\tilde{\varepsilon}} = \tilde{\boldsymbol{\varepsilon}}^\top &\left(\mathbf{R}_\mathrm{C}^\top \boldsymbol{\alpha}_\mathrm{v}^\mathrm{I} - \mathbf{v}_\mathrm{c}^\mathrm{C} + \mathbf{S}_\mathrm{C}^\top \boldsymbol{\varepsilon}_\mathrm{f} - \dot{\boldsymbol{\varepsilon}}_\mathrm{f}\right) + \\
&\tilde{\boldsymbol{\varepsilon}}^\top \mathbf{R}_\mathrm{C}^\top \mathbf{z}_\mathrm{v}^\mathrm{I}
\end{aligned} \tag{21}$$

when we employ $\mathbf{z}_\mathrm{v}^\mathrm{I} \triangleq \mathbf{v}^\mathrm{I} - \boldsymbol{\alpha}_\mathrm{v}^\mathrm{I}$, where $\boldsymbol{\alpha}_\mathrm{v}^\mathrm{I}$ represents the desired (ideal) linear velocity of the ship decomposed in **I**.

We now introduce a (virtual) *mediator* point located at $\mathbf{p}_\mathrm{m}$, which is defined such that when the ship converges to its assigned formation position relative to the path, the mediator converges to the path. Hence, $\boldsymbol{\varepsilon}_\mathrm{m} = \tilde{\boldsymbol{\varepsilon}}$. The relationship between the ship, the mediator, and the collaborator is illustrated in Figure 2, and can be expressed by

$$\begin{aligned}
\boldsymbol{\varepsilon} &= \boldsymbol{\varepsilon}_\mathrm{m} + \boldsymbol{\varepsilon}_\mathrm{f} && (22)\\
&= \mathbf{R}_\mathrm{C}^\top (\mathbf{p}_\mathrm{m} - \mathbf{p}_\mathrm{c}) + \boldsymbol{\varepsilon}_\mathrm{f} && (23)\\
&= \mathbf{R}_\mathrm{C}^\top (\mathbf{p} - \mathbf{p}_\mathrm{c}) && (24)
\end{aligned}$$

such that

$$\mathbf{p}_\mathrm{m} = \mathbf{p} - \mathbf{R}_\mathrm{C}\boldsymbol{\varepsilon}_\mathrm{f}, \tag{25}$$

which is used to compute (and continuously update) the location of the mediator.

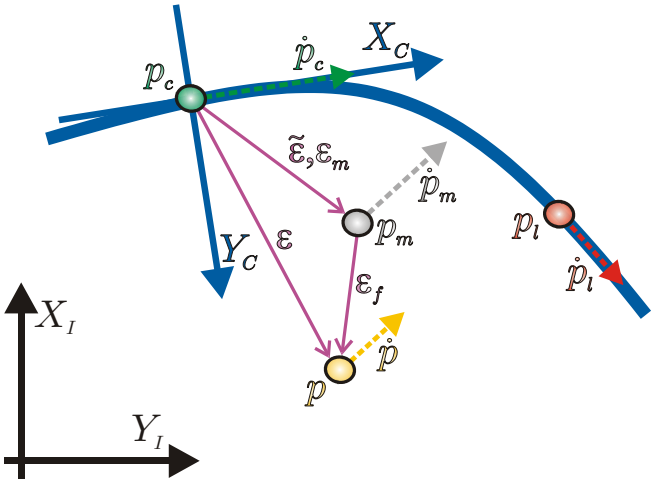

Fig. 2. The geometric relationship between the formation member ($\mathbf{p}$; orange), the mediator ($\mathbf{p}_\mathrm{m}$; grey), the collaborator ($\mathbf{p}_\mathrm{c}$; green), and the virtual leader ($\mathbf{p}_\mathrm{l}$; red). All the involved participants are virtual, except the formation member (ship). The role of the mediator is to facilitate (singularity-free) off-path traversing of curved paths.

Hence,

$$\dot{\mathbf{p}}_\mathrm{m} = \dot{\mathbf{p}} - \dot{\mathbf{R}}_\mathrm{C}\boldsymbol{\varepsilon}_\mathrm{f} - \mathbf{R}_\mathrm{C}\dot{\boldsymbol{\varepsilon}}_\mathrm{f},$$

which is equal to

$$\mathbf{v}_\mathrm{m}^\mathrm{I} = \mathbf{v}^\mathrm{I} - \mathbf{R}_\mathrm{C}\mathbf{S}_\mathrm{C}\boldsymbol{\varepsilon}_\mathrm{f} - \mathbf{R}_\mathrm{C}\dot{\boldsymbol{\varepsilon}}_\mathrm{f}, \tag{26}$$

entailing that

$$\boldsymbol{\alpha}_\mathrm{v,m}^\mathrm{I} = \boldsymbol{\alpha}_\mathrm{v}^\mathrm{I} - \mathbf{R}_\mathrm{C}\mathbf{S}_\mathrm{C}\boldsymbol{\varepsilon}_\mathrm{f} - \mathbf{R}_\mathrm{C}\dot{\boldsymbol{\varepsilon}}_\mathrm{f}, \tag{27}$$

or rather, that

$$\boldsymbol{\alpha}_\mathrm{v}^\mathrm{I} = \boldsymbol{\alpha}_\mathrm{v,m}^\mathrm{I} + \mathbf{R}_\mathrm{C}(\mathbf{S}_\mathrm{C}\boldsymbol{\varepsilon}_\mathrm{f} + \dot{\boldsymbol{\varepsilon}}_\mathrm{f}), \tag{28}$$

which we duly insert into (21) to achieve

$$\dot{V}_{\tilde{\varepsilon}} = \tilde{\boldsymbol{\varepsilon}}^\top \left(\mathbf{R}_\mathrm{C}^\top \boldsymbol{\alpha}_\mathrm{v,m}^\mathrm{I} - \mathbf{v}_\mathrm{c}^\mathrm{C}\right) + \tilde{\boldsymbol{\varepsilon}}^\top \mathbf{R}_\mathrm{C}^\top \mathbf{z}_\mathrm{v}^\mathrm{I} \tag{29}$$

since $\mathbf{S}_\mathrm{C} = -\mathbf{S}_\mathrm{C}^\top$. We note that $\boldsymbol{\alpha}_\mathrm{v,m}^\mathrm{I}$ represents the desired linear velocity of the mediator (that corresponds to the desired linear velocity of the ship) decomposed in **I**.

Subsequently, define $\boldsymbol{\alpha}_\mathrm{v,m}^\mathrm{I} \triangleq \mathbf{R}_\mathrm{DV}\boldsymbol{\alpha}_\mathrm{v,m}^\mathrm{DV}$, where $\boldsymbol{\alpha}_\mathrm{v,m}^\mathrm{DV} = [U_\mathrm{d,m}, 0]^\top$ ($U_\mathrm{d,m} = |\boldsymbol{\alpha}_\mathrm{v,m}^\mathrm{I}|$) represents the desired linear velocity of the mediator decomposed in a DESIRED VELOCITY frame (**DV**), i.e., decomposed along the desired velocity itself. Thus,

$$\begin{aligned}
\dot{V}_{\tilde{\varepsilon}} &= \tilde{\boldsymbol{\varepsilon}}^\top \left(\mathbf{R}_\mathrm{C}^\top \mathbf{R}_\mathrm{DV} \boldsymbol{\alpha}_\mathrm{v,m}^\mathrm{DV} - \mathbf{v}_\mathrm{c}^\mathrm{C}\right) + \tilde{\boldsymbol{\varepsilon}}^\top \mathbf{R}_\mathrm{C}^\top \mathbf{z}_\mathrm{v}^\mathrm{I} \\
&= \tilde{\boldsymbol{\varepsilon}}^\top \left(\mathbf{R}_\mathrm{R} \boldsymbol{\alpha}_\mathrm{v,m}^\mathrm{DV} - \mathbf{v}_\mathrm{c}^\mathrm{C}\right) + \tilde{\boldsymbol{\varepsilon}}^\top \mathbf{R}_\mathrm{C}^\top \mathbf{z}_\mathrm{v}^\mathrm{I}
\end{aligned}$$

where $\mathbf{R}_\mathrm{C}^\top \mathbf{R}_\mathrm{DV} \triangleq \mathbf{R}_\mathrm{R}$ represents the relative orientation between **C** and **DV**. Denote the corresponding angular difference by $\chi_\mathrm{r} \triangleq \chi_\mathrm{d} - \chi_\mathrm{c}$, and expand the CLF derivative to obtain

$$\dot{V}_{\tilde{\varepsilon}} = \tilde{s}(U_\mathrm{d,m}\cos\chi_\mathrm{r} - U_\mathrm{c}) + \tilde{e}U_\mathrm{d,m}\sin\chi_\mathrm{r} + \tilde{\boldsymbol{\varepsilon}}^\top \mathbf{R}_\mathrm{C}^\top \mathbf{z}_\mathrm{v}^\mathrm{I}.$$

Hence, U_c and χ_r can be considered as virtual inputs for driving $\tilde{\boldsymbol{\varepsilon}}$ to zero, given that $U_\mathrm{d,m} > 0$. Then, choose U_c as

$$U_\mathrm{c} = U_\mathrm{d,m}\cos\chi_\mathrm{r} + \gamma\tilde{s} \tag{30}$$

with $\gamma > 0$ constant, and χ_r as the helmsman-like

$$\chi_\mathrm{r} = \arctan\left(-\frac{\tilde{e}}{\triangle_{\tilde{e}}}\right) \tag{31}$$

with $\triangle_{\tilde{e}} > 0$ (not necessarily constant; a variable that is often referred to as a lookahead distance in literature treating planar path following along straight lines, see, e.g., (Papoulias 1991)), giving

$$\dot{V}_{\tilde{\varepsilon}} = -\gamma \hat{s}^2 - U_{\mathrm{d,m}} \frac{\tilde{e}^2}{\sqrt{\tilde{e}^2 + \triangle_{\tilde{e}}^2}} + \tilde{\boldsymbol{\varepsilon}}^\top \mathbf{R}_{\mathrm{C}}^\top \mathbf{z}_{\mathrm{v}}^{\mathrm{I}}, \tag{32}$$

which means that

$$\dot{\varpi}_{\mathrm{c}} = \frac{U_{\mathrm{c}}}{|\mathbf{p}_{\mathrm{c}}'|} \tag{33}$$

and

$$\chi_{\mathrm{d}} = \chi_{\mathrm{c}} + \chi_{\mathrm{r}}, \tag{34}$$

with U_{c} as in (30), χ_{c} as in (19), and χ_{r} as in (31). Equations (33) and (34) indicate that the collaborator continuously leads the mediator (which moves according to the ship), while the desired linear velocity of the mediator must point toward the path-tangential associated with the collaborator, in the direction of forward motion.

Summing up the design so far, we have introduced two virtual participants whose purposes are to guide the ship toward its assigned path-relative formation position. The use of the collaborator and the mediator ensure that possible kinematic singularities related to curved paths are avoided. They both move according to the ship, but their locations are used to calculate the desired orientation of the ship linear velocity required for converging to the specified formation position relative to the path.

In particular, the desired linear velocity of the ship is calculated from

$$\boldsymbol{\alpha}_{\mathrm{v}}^{\mathrm{I}} = \mathbf{R}_{\mathrm{DV}} \boldsymbol{\alpha}_{\mathrm{v,m}}^{\mathrm{DV}} + \mathbf{R}_{\mathrm{C}} (\mathbf{S}_{\mathrm{C}} \boldsymbol{\varepsilon}_{\mathrm{f}} + \dot{\boldsymbol{\varepsilon}}_{\mathrm{f}}) \tag{35}$$

since

$$\boldsymbol{\alpha}_{\mathrm{v}}^{\mathrm{I}} = \mathbf{R}_{\mathrm{DB}} \boldsymbol{\alpha}_{\mathrm{v}}^{\mathrm{DB}}, \tag{36}$$

where $\boldsymbol{\alpha}_{\mathrm{v}}^{\mathrm{DB}} = [U_{\mathrm{d}}, 0]^\top$ ($U_{\mathrm{d}} = |\boldsymbol{\alpha}_{\mathrm{v}}^{\mathrm{I}}|$) represents the desired linear velocity of the ship decomposed in a DESIRED BODY frame (**DB**), and

$$\mathbf{R}_{\mathrm{DB}} \triangleq \begin{bmatrix} \cos\chi_{\mathrm{d}} & -\sin\chi_{\mathrm{d}} \\ \sin\chi_{\mathrm{d}} & \cos\chi_{\mathrm{d}} \end{bmatrix} \tag{37}$$

represents the associated rotation matrix. Furthermore, define

$$\mathbf{H} \triangleq \begin{bmatrix} 1 & 0 & 0 \\ 0 & 1 & 0 \end{bmatrix}, \tag{38}$$

giving

$$\mathbf{R}_{\mathrm{B}} \triangleq \mathbf{H} \mathbf{R}(\psi) \mathbf{H}^\top \tag{39}$$

$$= \begin{bmatrix} \cos\psi & -\sin\psi \\ \sin\psi & \cos\psi \end{bmatrix}, \tag{40}$$

which can be used to state the relationship

$$\boldsymbol{\alpha}_{\mathrm{v}}^{\mathrm{I}} = \mathbf{R}_{\mathrm{B}} \boldsymbol{\alpha}_{\mathrm{v}}, \tag{41}$$

i.e.,

$$\boldsymbol{\alpha}_{\mathrm{v}} = \mathbf{R}_{\mathrm{B}}^\top \boldsymbol{\alpha}_{\mathrm{v}}^{\mathrm{I}}. \tag{42}$$

Hence, we also get

$$\mathbf{z}_{\mathrm{v}}^{\mathrm{I}} = \mathbf{R}_{\mathrm{B}} \mathbf{H} \mathbf{z}_{\nu}, \tag{43}$$

such that the system dynamics of $\tilde{\boldsymbol{\varepsilon}}$ and $\mathbf{z}_{\mathrm{g}}$ can be expressed as

$$\Sigma_1 : \dot{\tilde{\boldsymbol{\varepsilon}}} = \mathbf{f}_1(t, \tilde{\boldsymbol{\varepsilon}}) + \mathbf{g}_1(t) \mathbf{z}_{\mathrm{g}} \tag{44}$$

$$\Sigma_2 : \dot{\mathbf{z}}_{\mathrm{g}} = \mathbf{f}_2(t, \mathbf{z}_{\mathrm{g}}), \tag{45}$$

which is a pure cascade where the control subsystem ($\mathbf{z}_{\mathrm{g}}$) perturbs the guidance subsystem ($\tilde{\boldsymbol{\varepsilon}}$) through the interconnection matrix

$$\mathbf{g}_1(t) = \left[\mathbf{0}_{2\times 1}, \mathbf{R}_{\mathrm{C}}^\top \mathbf{R}_{\mathrm{B}} \mathbf{H}, \mathbf{0}_{2\times 3} \right]. \tag{46}$$

Now, consider the following assumptions:

A.1 $|\mathbf{p}_{\mathrm{p}}'| \in \left[|\mathbf{p}_{\mathrm{p}}'|_{\min}, \infty \right\rangle \; \forall \varpi \in \mathbb{R}$, $|\mathbf{p}_{\mathrm{p}}'|_{\min} > 0$

A.2 $\triangle_{\tilde{\mathrm{e}}} \in [\triangle_{\tilde{\mathrm{e}},\,\min}, \infty\rangle$, $\triangle_{\tilde{\mathrm{e}},\,\min} > 0$

A.3 $U_{\mathrm{d,m}} \in [U_{\mathrm{d,m,min}}, \infty\rangle$, $U_{\mathrm{d,m,min}} > 0$

Assumption A.1 means that the geometric path must be regularly parameterized, assumption A.2 implies that the linear velocity of the mediator must be directed toward the path-tangential, while assumption A.3 represents a minimum-speed requirement for the desired mediator linear velocity.

By contemplating $\boldsymbol{\xi} \triangleq \left[\tilde{\boldsymbol{\varepsilon}}^\top, \mathbf{z}_{\mathrm{g}}^\top \right]^\top$, we arrive at:

Proposition 2. The equilibrium point $\boldsymbol{\xi} = \mathbf{0}$ is rendered uniformly globally asymptotically and locally exponentially stable (UGAS/ULES) under assumptions A.1-A.3 when applying (13-14) with the reference signals (12) and (42).

Proof. Since the origin of system Σ_2 is shown to be UGAS/ULES in Proposition 1, the origin of the unperturbed system Σ_1 (i.e., when $\mathbf{z}_{\mathrm{g}} = \mathbf{0}$) is trivially shown to be UGAS/ULES by applying standard Lyapunov theory to (16) and (32), and the interconnection term satisfies $|\mathbf{g}_1(t)| = 1$, the proposed result follows directly from Theorem 7 and Lemma 8 of (Panteley *et al.* 1998). ■

So far, the two first design steps has made it possible for each individual ship to converge to and maintain its assigned formation position relative to the assigned path. The final design step must deal with the synchronization of each formation member with the virtual formation leader, i.e., ensuring the assembly of the formation as a whole.

Step 3: Synchronization Loop Design In this final design step, we determine the required *size* of $\boldsymbol{\alpha}_{\mathrm{v}}$, derived indirectly through $U_{\mathrm{d,m}}$, such that a ship controlled by (13) and (14) with reference signals given by (12) and (42) synchronizes with the formation leader.

Consequently, consider the positive definite and radially unbounded CLF

$$V_{\tilde{\varpi}} \triangleq \frac{1}{2} \tilde{\varpi}^2, \tag{47}$$

where

$$\tilde{\varpi} \triangleq \varpi_{\mathrm{c}} - \varpi_{\mathrm{l}}, \tag{48}$$

and differentiate the CLF with respect to time to get

$$\begin{aligned} \dot{V}_{\tilde{\varpi}} &= \tilde{\varpi} \dot{\tilde{\varpi}} \\ &= \tilde{\varpi} (\dot{\varpi}_{\mathrm{c}} - \dot{\varpi}_{\mathrm{l}}) \\ &= \tilde{\varpi} (z_{\mathrm{c}} + \alpha_{\mathrm{c}} - \dot{\varpi}_{\mathrm{l}}), \end{aligned}$$

where $z_{\mathrm{c}} \triangleq \dot{\varpi}_{\mathrm{c}} - \alpha_{\mathrm{c}}$, and α_{c} represents the desired speed of the collaborator when the mediator has converged to the path, i.e., when $\boldsymbol{\xi} = \mathbf{0}$. Hence, we have that

$$\dot{V}_{\tilde{\varpi}} = \tilde{\varpi}\left(\frac{U_{\mathrm{d,m}}}{|\mathbf{p}_{\mathrm{c}}'|} - \frac{U_{\mathrm{l}}}{|\mathbf{p}_{\mathrm{l}}'|}\right) + \tilde{\varpi} z_{\mathrm{c}},$$

which becomes equal to

$$\dot{V}_{\tilde{\varpi}} = -k_{\tilde{\varpi}} \frac{\tilde{\varpi}^2}{\sqrt{\tilde{\varpi}^2 + \triangle_{\tilde{\varpi}}^2}} + \tilde{\varpi} z_{\mathrm{c}} \tag{49}$$

when choosing

$$U_{\mathrm{d,m}} = |\mathbf{p}_{\mathrm{c}}'|\left(\frac{U_{\mathrm{l}}}{|\mathbf{p}_{\mathrm{l}}'|} - k_{\tilde{\varpi}} \frac{\tilde{\varpi}}{\sqrt{\tilde{\varpi}^2 + \triangle_{\tilde{\varpi}}^2}}\right), \tag{50}$$

where $\triangle_{\tilde{\varpi}} \in [\triangle_{\tilde{\varpi},\,\min}, \infty\rangle$, $\triangle_{\tilde{\varpi},\,\min} > 0$, and where

$$k_{\tilde{\varpi}} = \sigma \frac{U_{\mathrm{l}}}{|\mathbf{p}_{\mathrm{l}}'|},\ \sigma \in \langle 0, 1] \tag{51}$$

ensures that $U_{\mathrm{d,m}}$ satisfies Assumption A.3 since

$$U_{\mathrm{d,m}} = U_{\mathrm{l}}\left(1 - \sigma \frac{\tilde{\varpi}}{\sqrt{\tilde{\varpi}^2 + \triangle_{\tilde{\varpi}}^2}}\right)\frac{|\mathbf{p}_{\mathrm{c}}'|}{|\mathbf{p}_{\mathrm{l}}'|}. \tag{52}$$

Then, expand z_{c} to get

$$\begin{aligned} z_{\mathrm{c}} &= \dot{\varpi}_{\mathrm{c}} - \alpha_{\mathrm{c}} \\ &= \frac{U_{\mathrm{d,m}}(\cos\chi_{\mathrm{r}} - 1) + \gamma \tilde{s}}{|\mathbf{p}_{\mathrm{c}}'|}, \end{aligned} \tag{53}$$

where

$$(\cos\chi_{\mathrm{r}} - 1) = \frac{\triangle_{\tilde{\mathrm{e}}} - \sqrt{\tilde{e}^2 + \triangle_{\tilde{\mathrm{e}}}^2}}{\sqrt{\tilde{e}^2 + \triangle_{\tilde{\mathrm{e}}}^2}}, \tag{54}$$

such that the system dynamics of $\tilde{\varpi}$ and $\boldsymbol{\xi}$ can be written

$$\Sigma_3 : \dot{\tilde{\varpi}} = f_3(t, \tilde{\varpi}) + \mathbf{g}_3(t, \boldsymbol{\xi})^{\top}\boldsymbol{\xi} \tag{55}$$

$$\Sigma_4 : \dot{\boldsymbol{\xi}} = \mathbf{f}_4(t, \boldsymbol{\xi}), \tag{56}$$

which is a cascaded system where the synchronization subsystem ($\tilde{\varpi}$) is perturbed through the interconnection vector

$$\mathbf{g}_3(t, \boldsymbol{\xi}) = \frac{1}{|\mathbf{p}_{\mathrm{c}}'|}\left[\gamma, U_{\mathrm{d,m}} \frac{\triangle_{\tilde{\mathrm{e}}} - \sqrt{\tilde{e}^2 + \triangle_{\tilde{\mathrm{e}}}^2}}{\tilde{e}\sqrt{\tilde{e}^2 + \triangle_{\tilde{\mathrm{e}}}^2}}, \mathbf{0}_{1\times 2}\right]^{\top}, \tag{57}$$

which is well-defined since

$$\lim_{\tilde{e}\to 0} \frac{\triangle_{\tilde{\mathrm{e}}} - \sqrt{\tilde{e}^2 + \triangle_{\tilde{\mathrm{e}}}^2}}{\tilde{e}\sqrt{\tilde{e}^2 + \triangle_{\tilde{\mathrm{e}}}^2}} = 0. \tag{58}$$

Note that the complete cascade structure is completely modular in the sense that the control subsystem ($\mathbf{z}_{\mathrm{g}}$) excites the guidance subsystem ($\tilde{\boldsymbol{\varepsilon}}$), which in turn excites the synchronization subsystem ($\tilde{\varpi}$).

By considering $\boldsymbol{\zeta} \triangleq \left[\tilde{\varpi}, \boldsymbol{\xi}^{\top}\right]^{\top}$, we can now state the following main theorem:

Theorem 1. The equilibrium point $\boldsymbol{\zeta} = \mathbf{0}$ is rendered UGAS/ULES under assumptions A.1-A.2 when applying (13-14) with reference signals (12) and (42) employing (52).

Proof. Since the origin of system Σ_4 is shown to be UGAS/ULES in Proposition 2, the origin of the unperturbed system Σ_3 (i.e., when $\boldsymbol{\xi} = \mathbf{0}$) is trivially shown to be UGAS/ULES by applying standard Lyapunov theory to (47) and (49), and the interconnection term satisfies $|\mathbf{g}_3(t, \boldsymbol{\xi})| < |\mathbf{p}_{\mathrm{p}}'|_{\min}^{-1}\left(\gamma^2 + \left(\frac{U_{\mathrm{l,max}}}{\triangle_{\tilde{\mathrm{e}},\,\min}}\right)^2\right)^{1/2}$, the proposed result follows directly from Theorem 7 and Lemma 8 of (Panteley *et al.* 1998). ■

If every formation member satisfies the conditions of Theorem 1, the formation control problem (6) is solved.

3. DISCUSSION

The guided scheme can also be extended to handle underactuated ships due to its output space of linear velocity and heading, where the heading can either be independently controlled (fully actuated case) or dedicated to control the orientation of the linear velocity (underactuated case). Hence, keeping the control subsystem unchanged, a purposeful redesign of the guidance and synchronization subsystems enables underactuated operations. In fact, when the scenario entails straight-line paths and no environmental disturbances, a redesign is not necessary if

$$\psi_{\mathrm{d}} = \chi_{\mathrm{d}}, \tag{59}$$

i.e., the desired heading is assigned as the desired orientation of the linear velocity.

The specific version of the guided scheme that has been presented in this paper is decentralized in the sense that no coordination variables are communicated between the formation members. Hence, the loop is open at the leader-follower level, i.e., the leader propagates without feedback from the followers. Consequently, while impervious to single-point failure, the formation suffers from graceful degradation, i.e., members who cannot keep up with the leader fall out of formation. However, they will still be able to follow their assigned formation positions relative to the path. Thus, this decentralized scheme could be classified as involving tactical (i.e., local/individual) path following, but strategic (i.e., global/formation-wide) trajectory tracking. An alternative solution involves path following at both the tactical and strategic levels, where the leader receives formation-wide feedback from the followers (perhaps applying such information through a consensus-based algorithm). Hence, strategic path following values spatial aspects over temporal requirements (i.e., the most important task is to maintain the formation composition), while the opposite is true for strategic trajectory tracking (i.e., the formation composition can be sacrificed if some of the members cannot satisfy their required temporal constraints). Strategic trajectory tracking would typically be chosen for dedicated military operations since such endeavors usually have tight temporal constraints and inherently involve radio silence.

4. CASE STUDY: FULLY ACTUATED SHIPS

To illustrate the transient motion behavior associated with the proposed scheme, a computer simulation is carried out in which three fully actuated ships assemble and maintain a V-shaped formation along a sinusoidal path while being exposed to a constant environmental force. Specifically, the desired path is parameterized as $x_{\mathrm{p}}(\varpi) = 10\sin(0.1\varpi)$ $[m]$ and $y_{\mathrm{p}}(\varpi) = \varpi$ $[m]$; the environmental force acts from due north with a size of 1 N; the ship parameters are taken from Cybership 2, a 1:70 scale model of an offshore

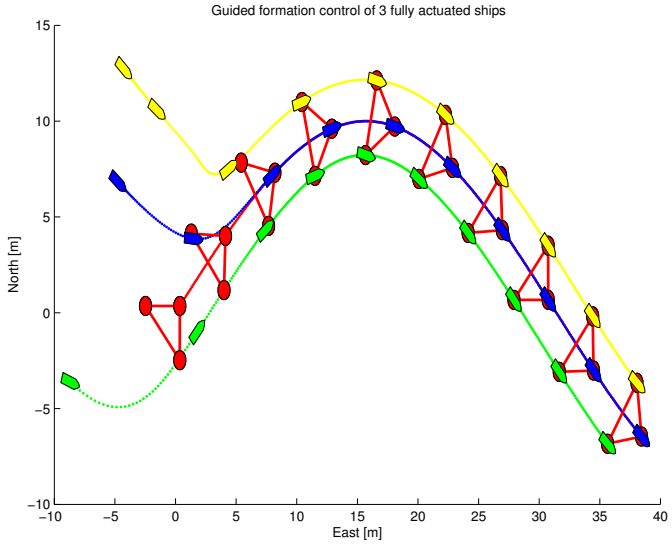

Fig. 3. The transient motion behavior of 3 fully actuated ships that assemble and maintain a V-shaped formation along a sinusoid while exposed to a constant environmental disturbance acting from the north.

supply vessel (Skjetne *et al.* 2004); the control gains and parameters are chosen as $k_{\psi,\mathrm{i}} = 10$, $\mathbf{K}_{\nu,\mathrm{i}} = 10\mathbf{I}$, $\mathbf{\Gamma}_\mathrm{i} = \mathbf{I}$, $\gamma_\mathrm{i} = 100$, $\triangle_{\mathrm{e,i}} = \triangle_{\tilde{\varpi},\mathrm{i}} = 1$ and $\sigma_\mathrm{i} = 0.9$, $\forall i \in \mathcal{I} = \{1, 2, 3\}$; and the speed of the virtual leader is fixed at $U_\mathrm{l} = 0.25$ $[m/s]$. Figure 3 illustrates the transient behavior of the formation members as they assemble and maintain a V-shaped formation defined by $\boldsymbol{\varepsilon}_{\mathrm{f},1} = [-2, -2]^\top$, $\boldsymbol{\varepsilon}_{\mathrm{f},2} = [0, 0]^\top$ and $\boldsymbol{\varepsilon}_{\mathrm{f},3} = [-2, 2]^\top$.

5. CONCLUSIONS

This paper has addressed the topic of formation control for fully actuated ships. A guided formation control concept was developed within a leader-follower framework by means of a modular design procedure, inspired by integrator backstepping and theory on nonlinear time-varying cascades. The three-step design procedure involved the creation of control, guidance, and synchronization laws for each formation member. Also, a key novelty of the approach was the derivation of guidance laws applicable to off-path traversing of curved paths. The helmsman-like transient motion behavior associated with the scheme was finally illustrated through a computer simulation involving three fully actuated ships.

REFERENCES

Aguiar, A. P., R. Ghabcheloo, A. Pascoal, C. Silvestre, J. Hespanha and I. Kaminer (2006). Coordinated path-following of multiple underactuated autonomous vehicles with bidirectional communication constraints. In: *Proceedings of the ISCCSP'06, Marrakech, Morocco.*

Arrichiello, F., S. Chiaverini and T. I. Fossen (2006). Formation control of underactuated surface vessels using the null-space-based behavioral control. In: *Proceedings of the IROS'06, Beijing, China.*

Breivik, M., M. V. Subbotin and T. I. Fossen (2006). Guided formation control for wheeled mobile robots. In: *Proceedings of the 9th ICARCV, Singapore.*

Encarnação, P. and A. Pascoal (2001). Combined trajectory tracking and path following: An application to the coordinated control of autonomous marine craft. In: *Proceedings of the 40th IEEE CDC, Orlando, Florida, USA.*

Fiorelli, E., N. E. Leonard, P. Bhatta, D. Paley, R. Bachmayer and D. M. Fratantoni (2004). Multi-AUV control and adaptive sampling in Monterey Bay. In: *Proceedings of the AUV'04, Sebasco, Maine, USA.*

Fossen, T. I. (2002). *Marine Control Systems: Guidance, Navigation and Control of Ships, Rigs and Underwater Vehicles.* Marine Cybernetics.

Fossen, T. I., A. Loría and A. Teel (2001). A theorem for UGAS and ULES of (passive) nonautonomous systems: Robust control of mechanical systems and ships. *International Journal of Robust and Nonlinear Control* **11**, 95–108.

Fossen, T. I., M. Breivik and R. Skjetne (2003). Line-of-sight path following of underactuated marine craft. In: *Proceedings of the 6th IFAC MCMC, Girona, Spain.*

Ihle, I.-A. F., J. Jouffroy and T. I. Fossen (2005). Formation control of marine surface craft using Lagrange multipliers. In: *Proceedings of the 44th IEEE CDC, Seville, Spain.*

Krstić, M., I. Kanellakopoulos and P. V. Kokotović (1995). *Nonlinear and Adaptive Control Design.* John Wiley & Sons Inc.

Kumar, V., Leonard, N. E. and Morse, A. S., Eds.) (2005). *Cooperative Control.* Vol. 309 of *Lecture Notes in Control and Information Sciences.* Springer-Verlag.

Kyrkjebø, E. and K. Y. Pettersen (2006). Leader-follower dynamic synchronization of surface vessels. In: *Proceedings of the 7th IFAC MCMC, Lisbon, Portugal.*

Lapierre, L., D. Soetanto and A. Pascoal (2003). Coordinated motion control of marine robots. In: *Proceedings of the 6th IFAC MCMC, Girona, Spain.*

Panteley, E., E. Lefeber, A. Loría and H. Nijmeijer (1998). Exponential tracking of a mobile car using a cascaded approach. In: *Proceedings of the IFAC Workshop on Motion Control, Grenoble, France.*

Papoulias, F. A. (1991). Bifurcation analysis of line of sight vehicle guidance using sliding modes. *International Journal of Bifurcation and Chaos* **1**(4), 849–865.

Pavlov, A., E. Børhaug, E. Panteley and K.Y. Pettersen (2007). Straight line path following for formations of underactuated surface vessels. In: *Proceedings of the 7th IFAC NOLCOS, Pretoria, South Africa.*

Pettersen, K. Y., Gravdahl, J. T. and Nijmeijer, H., Eds.) (2006). *Group Coordination and Cooperative Control.* Vol. 336 of *Lecture Notes in Control and Information Sciences.* Springer-Verlag.

Skjetne, R., Ø. N. Smogeli and T. I. Fossen (2004). A nonlinear ship manoeuvering model: Identification and adaptive control with experiments for a model ship. *Modeling, Identification and Control* **25**(1), 3–27.

Skjetne, R., S. Moi and T. I. Fossen (2002). Nonlinear formation control of marine craft. In: *Proceedings of the 41st IEEE CDC, Las Vegas, Nevada, USA.*

Sørdalen, O. J. and O. Egeland (1995). Exponential stabilization of nonholonomic chained systems. *IEEE Transactions on Automatic Control* **40**(1), 35–49.